COMPOSITION AND SIZE DEPENDENT ABRASION OF A ROCK ON THE MOON DERIVED FROM TOPOGRAPHIC DIFFUSION MODELING AND OPTICAL OBSERVATIONS. O. Ruesch[1] and C. Wöhler[2], [1]Institut für Planetologie, Westfälische Wilhelms Universität Münster, Münster, Germany (ottaviano.ruesch@uni-muenster.de), [2]Image Analysis Group, Technische Universität Dortmund, Dortmund, Germany.

Introduction: There is a need to understand regolith evolution on airless surfaces at the local scale, i.e., at a spatial scale below the tens of meters. Knowledge of regolith at this scale is relevant for all investigations by lunar [e.g., 1] and asteroid in situ missions [e.g., 2,3]. The concept of this study is to extract information on regolith evolution from single instances of blocks (i.e., rootless rock in the range 1-100 m) resting on the surface of the Moon. Blocks are the result of impact ejecta and mass wasting processes. Once exposed on the surface, they are subject to a variety of erosional processes [4]. For the spatial scale of interest, the most dominant erosion mechanism is shattering by meteoroids and abrasion by micrometeoroids [5]. Fassett and Thomson [6] demonstrated how the diffusive process of micrometeoroids abrasion can be modeled to derive age information for large craters. Here we take the same approach to model the topographic evolution of blocks driven solely by abrasion. Although both shattering and abrasion occur on blocks, instances where only the effect of abrasion is evident (i.e., absence of shattering) are abundant [e.g., 7]. Age and compositional information is mined by coupling the model topography to optical images acquired in situ.

Method: Modeling of the topographic evolution aims at reproducing key morphological properties of blocks: (i) roundness at block edges, (ii) embankment of the block by loose fine-grained material, i.e., fillet, (iii) fillet onlap on the block. The modeling consists of two major steps:

(1) We approximate the erosion of the block by considering micrometeoroid abrasion as a diffusive process [8, 9]. The diffusivity coefficient (k_{block}) is set as a free parameter to reflect different block strengths. The parameter k_{block} is a function of block size, as proposed for craters in [10]. In addition to diffusion, mass wasting by advection can occur on the steep sides, in particular for fresh blocks. This additional type of erosional mechanism is not considered because it does not dominate over the time scale of the simulations [e.g., 11,12]. The initial topography of a block is set as a rectangular cuboid with axes a, b and c defined as b/a=0.8 and c/a=0.54 as observed on the Moon [13].

(2) All mass removed from the block is deposited next to it and constitutes the fillet. The fillet itself is allowed to diffuse due to micrometeoroid abrasion with a diffusivity coefficient k_{fillet}. Because the fillet is composed of loose material and the block is coherent, we set $k_{fillet}>k_{block}$. The parameter k_{fillet} is also a function of fillet size.

Results: Examples of modelled topographic profiles for two blocks of different strengths are shown in Figure 1. Clearly, the height of the fillet is greater for a block of lower strength, independently of surface exposure time. We determined the values of k_{fillet} and k_{block} for a range of block strengths and sizes by fitting the topographic profile derived by the model to actual reference blocks. These reference blocks are instances where the exposure age is known and a topographic profile can be measured from images. Figure 2 illustrates that the topographic model can reproduce the most important sections of a profile, namely the decrease of the fillet slope away from the block, the height of the fillet at the contact with the block, and the mean height of the block.

For blocks of similar sizes and similar c/a values at t=0, we find that two morphometrical parameters, the slope of the fillet and the ratio h_{fillet}/h_{block}, allow to disentangle the morphological trend due to increasing surface exposure age from the trend due to increasing block strength (Figure 3). Parameters h_{fillet} and h_{block} are the maximum height of the fillet and block, respectively. The ratio between block height and block width is relatively constant with time for moderately young (<~50 My) and coherent block and is thus less diagnostic. For 2 m sized blocks we find that only if their material is weak and rested on the surface for >100 My, a noticeable decrease of the ratio occurs.

Discussion and Conclusion: The results confirm Apollo-era suggestions that fillet development depends primarily on block coherence, original block shape and exposure age [14]. The possibility to disentangle age versus composition for a block of given size is due to a combination of effects, i.e., while fillets have a uniform diffusivity their growth is a function of the block diffusivity (growth depend on age and strength). It will be possible to estimate erosion rates as a function of block size and strength by including additional reference blocks observed from orbit. Block strength can be used as a proxy for block type (i.e.,

petrology), and thus composition: possible endmembers are igneous blocks for high strength blocks, and light matrix regolith breccias for low strength blocks [e.g., 15]. In future in situ missions, 3D time-of-flight cameras [e.g., 16, 17] might be used for surface-based topography reconstructions of blocks and smaller rocks.

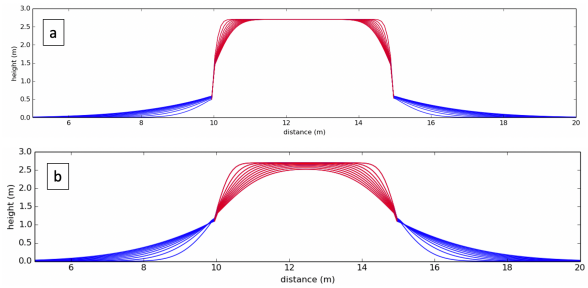

Figure 1. Example of modelled topographic profile for 5-m sized blocks from 10 My to 100 My of surface exposure age. Blue and red are the fillet and block sections, respectively. (a) A low diffusivity (high strength) block material. (b) A high diffusivity (low strength) block material.

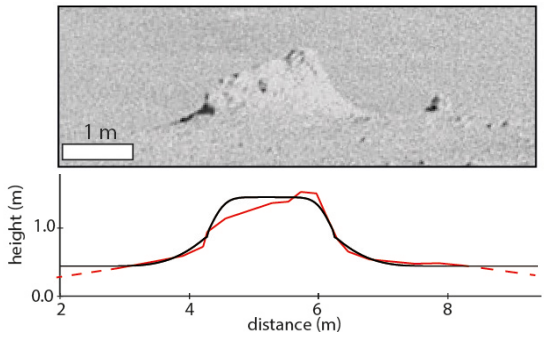

Figure 2. Block 1005 at Cone Crater, image AS14-68-9432HR, Apollo 14. The red and black profiles are the topographic profile extracted from the image above and the modelled profile, respectively.

Acknowledgments: O.R. is supported by a Sofja Kovalevskaja Award of the Alexander von Humboldt Foundation.

References: [1] Di, K., et al. (2016) PSS, 120, 103-112, doi:10.1016/j.pss.2015.11.012. [2] Jaumann, R., et al. (2019) Science, doi: 10.1126/science.aaw8627. [3] Murdoch, N. et al. (2020) Proc. EPSC, doi:10.5194/epsc2020-247. [4] Hoerz et al., (2020), PSS, doi:10.1016/j.pss.2020.105105. [5] Hoerz et al., (1977), Plus. Chem. Earth Vol. X. pp. 3 15.

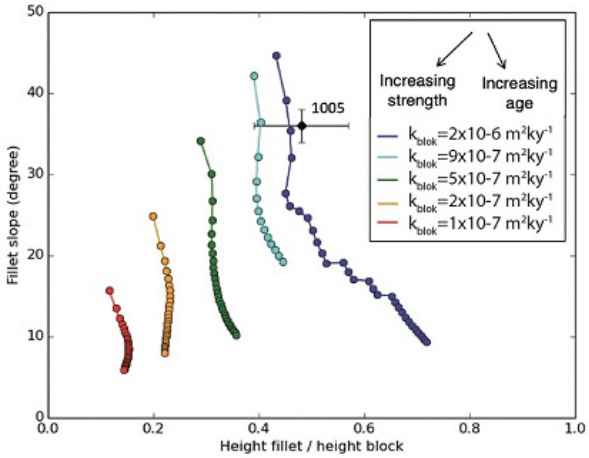

Figure 3. Morphological parameters measured on modelled blocks with fillets $k_{fillet}=2x10^{-6}$ m^2ky^{-1}. The simulated tracks start at the top at a surface exposure age of t=10 Ma, the time interval between subsequent points is 10 Ma. Trends due to increasing exposure age and increasing strength (different color) can be disentangled. The diamond symbol is the reference block 1005, 26 Ma in age [18] and 2 m in size, shown in Figure 2.

[6] Fassett, C. I. and Thomson, B. J. (2014) J. Geophys. Res., doi:10.1002/2014JE004698. [7] Ruesch, O., et al. (2020) Icarus, doi:10.1016/j.icarus.2019.113431. [8] Craddock, R. A., and Howard, A. D. (2000) J. Geophy. Res. 105(E8), 20,387-20,401. [9] Howard, A. D., (2007), Geomorphology, doi:10.1016/j.geomorph.2007.04.017. [10] Fassett, C. I. et al. (2018) LPSC, abstract #1502. [11] Roering, J. J. R., et al. (1999) Water Res. Res. 35(3), 853-870. [12] Minton, D. A. et al. (2019) Icarus, doi:10.1016/j.icarus.2019.02.021. [13] Demidov, N. W. and Basilevsky, A. T. (2014) SSR 48(5), 324-329. [14] Swann et al. (1972) Preliminary geologic investigation of the Apollo 15 landing site. NASA SP-289. [15] McGee, P. E. et al. (1979) Introduction to the Apollo collections: Part II lunar breccias, NASA. [16] Dziura, M., et al. (2017) IEEE Aerospace Conf., doi:10.1109/AERO.2017.7943679. [17] Gomez Martinez, H., et al. (2017) Acta Astronautica, doi:10.1016/j.actaastro.2017.07.002. [18] Arvidson, R., et al. (1975) The Moon 13, 259-276.